

# Windowing and Leakage in the Cross-Correlation Search for Periodic Gravitational Waves

Santosh Sundaresan and John T. Whelan

LIGO-T1200431-v1

Sun Sep 9 19:26:25 2012 -0400

## Abstract

We consider the impact of spectral leakage and windowing on the sensitivity of the cross-correlation search for periodic gravitational waves. We consider the modification to the expected signal-to-noise ratio ( $\propto h_0^2$ , so perhaps better thought of as SNR-squared) in the detection statistic relative to the naïve formula which assumes rectangular windows and signal frequency always in the center of an SFT bin. On average we expect the SNR associated with a search of rectangular-windowed data to be 77.4% of the naïve value. This is still better than the average expected from Hann-windowed data (60.1%) and data processed with a half-Hann/half-rectangular Tukey window (69.9%). Even though the Hann and Tukey windows leak a smaller fraction of their best-case SNR out of the best bin, the best-case scenarios are not as good—66.7% and 81.8%, respectively, of the naïve SNR is obtained even if the Doppler-shifted frequency always falls in the center of a bin. The sensitivity of the search can be improved by including contributions from multiple SFT bins. In general this requires accounting for correlations between bins, but for rectangularly-windowed data those correlations vanish and the combination is simpler, and results in an improvement of SNR from 77.4% to 90.3% of the naïve value when the two closest bins from each SFT are included in the search, and to 93.1% with the three closest bins. These values all come from an assumption that the sum over SFT pairs effects an average over the fractional offset of the signal frequency from the SFT bin center, an assumption which we investigate for several choices of search parameters.

## Contents

<b>1</b>	<b>Introduction</b>	<b>2</b>
<b>2</b>	<b>The cross-correlation method</b>	<b>2</b>
2.1	Short Fourier transforms . . . . .	2
2.2	Details of specific windows . . . . .	4
2.3	Signal cross-correlation . . . . .	7
2.4	Statistics of cross-correlation . . . . .	8
2.5	Optimal combination . . . . .	11

<b>3</b>	<b>Sensitivity estimates for different windowing options</b>	<b>12</b>
3.1	Naïve sensitivity . . . . .	12
3.2	Best-bin sensitivities . . . . .	12
3.2.1	Upper bound . . . . .	12
3.2.2	Averaged values . . . . .	13
3.3	Multiple-bin sensitivities . . . . .	14
3.4	Examples with specific parameter choices . . . . .	16
3.4.1	Caveats . . . . .	19

# 1 Introduction

Cross-correlation of Gravitational wave detector streams has been used to perform unmodelled searches for isolated astrophysical sources of Gravitational waves, treated as unmodelled stochastic sources. However, greater sensitivity can be achieved using a modelled cross-correlation search. We use this method to search for Gravitational Waves emitted from the Low-mass X-ray binary (LMXB) Scorpius X-1 (Sco X-1) as Sco X-1 is a rich source of Gravitational Waves. The Sco X-1 is a binary source in a known sky location with unknown frequency and residual uncertainty in the binary orbital parameters. The standard cross-correlation search looks for correlations between segments of data taken at the same or different times in the same or different gravitational wave detectors. By adjusting the maximum allowed offset time lag, one can achieve an optimum amount balance of sensitivity and computing cost. Since the signal is mostly monochromatic, the search cross correlates a single frequency bin in the Fourier transform of each detector, whose frequency is identified using the Doppler shift associated with the signal parameters (sky position, intrinsic frequency, spindown etc) and the properties of the detector response (location, orientation and velocity of the detector). But since this signal frequency is time dependent, we have to use finite time Fourier transforms.

The standard cross-correlation search for periodic gravitational waves [1, 2] presumes that the signal contribution comes from a single frequency bin in each SFT, and ignores the effects of windowing and leakage on that contribution. In reality, the signal contribution will be spread over several bins, and the details of that leakage will depend on whether and how the data were windowed before performing the Fourier transform. In this note we give a careful treatment to these effects, calculating the sensitivity of a search conducted with data subjected to different windows (rectangular, Hann, and Tukey), and compare this sensitivity to the naïve expression given in [1].

# 2 The cross-correlation method

## 2.1 Short Fourier transforms

The cross-correlation search, like most CW analyses, works with “Short Fourier Transforms” (SFTs). The data are divided into segments of length  $\Delta T$  and then Fourier transformed. We label an SFT with an index  $I$ , which refers to both the detector in question and the

timestamp  $T_I$  of the midpoint of the data segment used to construct the SFT. If the original timeseries data are sampled at a rate  $1/\delta t$ , the SFT is constructed as

$$\begin{aligned}\tilde{x}_{Ik} &= \sum_{j=0}^{N-1} x_{T_I j} e^{-i2\pi j k/N} \delta t = \sum_{j=0}^{N-1} x_I(T_I - \Delta T/2 + j \delta t) e^{-i2\pi j \delta t k/\Delta T} \delta t \\ &\approx e^{-i\pi f_k \Delta T} \int_{T_I - \Delta T/2}^{T_I + \Delta T/2} x_I(t) e^{-i2\pi f_k(t-T_I)} dt = (-1)^k \int_{T_I - \Delta T/2}^{T_I + \Delta T/2} x_I(t) e^{-i2\pi f_k(t-T_I)} dt\end{aligned}\quad (2.1)$$

where the frequency corresponding to the  $k$ th bin of the SFT is

$$f_k = k \delta f = \frac{k}{\Delta T} \quad (2.2)$$

In practice, the data are often multiplied by a window function  $w_j = w(j \delta t - T)$  before being Fourier transformed, so that (2.1) becomes

$$\tilde{x}_{Tk}^w = \sum_{j=0}^{N-1} w_j x_{Tj} e^{-i2\pi j k/N} \delta t \approx (-1)^k \int_{T - \Delta T/2}^{T + \Delta T/2} w(t - T) x(t) e^{-i2\pi f_k(t-T)} dt \quad (2.3)$$

When considering the signal contribution to a particular SFT, we use the fact that the signal model generates a signal which can be approximated as monochromatic over the duration of an SFT:

$$\begin{aligned}h_I(t) &= h_0 (F_+^I \mathcal{A}_+ \cos \Phi(\tau(t)) + F_\times^I \mathcal{A}_\times \sin \Phi(\tau(t))) \\ &\approx h_0 \{F_+^I \mathcal{A}_+ \cos(\Phi_I + 2\pi f_I[t - T_I]) + F_\times^I \mathcal{A}_\times \sin(\Phi_I + 2\pi f_I[t - T_I])\}\end{aligned}\quad (2.4)$$

where we have Taylor expanded the phase about the time  $T_I$ :

$$\Phi(\tau(t)) \approx \Phi_I + f_I(t - T_I) \quad (2.5)$$

The form of (2.4) includes the following parameters and definitions:

- $h_0$  is the intrinsic signal amplitude.
- $\mathcal{A}_+ = \frac{1+\cos^2 \iota}{2}$  and  $\mathcal{A}_\times = \cos \iota$  depend on the inclination  $\iota$  of the rotation axis to the line of sight.
- The antenna patterns  $F_+^I$  and  $F_\times^I$  depend on the detector in question, the sidereal time at  $T_I$ , the sky position  $\alpha, \delta$ , and the polarization angle  $\psi$ .
- The relationship  $\tau(t)$  between the SSB time and the time at the detector depends on the sky position and time.<sup>1</sup> Thus the phase  $\Phi(\tau(t))$  depends on time, detector,  $\Phi_0$ ,  $f_0, f_1, \dots$ , sky position and—in the case of a binary—the binary orbital parameters.

---

<sup>1</sup>Specifically, if  $\vec{r}_{\text{det}}$  is the position of the detector and  $\hat{k}$  is the unit vector pointing from the source to the SSB,  $\tau(t) \approx t - \vec{r}_{\text{det}} \cdot \hat{k}/c$ .

The signal contribution in bin  $k$  of the SFT  $I$ , if the data are not windowed, can be shown to be

$$\tilde{h}_{Ik} \approx h_0(-1)^k e^{i\Phi_I} \frac{F_+^I \mathcal{A}_+ - i F_\times^I \mathcal{A}_\times}{2} \delta_{\Delta T}(f_k - f_I) \quad (2.6)$$

where we have defined

$$\delta_{\Delta T}(f_k - f_I) = \int_{T-\Delta T/2}^{T+\Delta T/2} e^{-i2\pi(f_k - f_I)(t-T)} dt = \frac{\sin \pi(f_k - f_I)\Delta T}{\pi(f_k - f_I)} \quad (2.7)$$

which is a finite-time approximation of the Dirac delta function. If the data are windowed before constructing the SFTs, the signal contribution in bin  $k$  of SFT  $I$  is

$$\tilde{h}_{Ik}^w \approx h_0(-1)^k e^{i\Phi_I} \frac{F_+^I \mathcal{A}_+ - i F_\times^I \mathcal{A}_\times}{2} \delta_{\Delta T}^w(f_k - f_I) \quad (2.8)$$

where

$$\delta_{\Delta T}^w(f_k - f_I) = \int_{T-\Delta T/2}^{T+\Delta T/2} w(t-T) e^{-i2\pi(f_k - f_I)(t-T)} dt \quad (2.9)$$

Note that if  $w(t-T)$  has desirable properties like symmetry, monotonicity, and non-negativity, then  $\delta_{\Delta T}^w(\kappa \delta f)$  will be real and symmetric, and have a maximum value of

$$\delta_{\Delta T}^w(0) = \int_{T-\Delta T/2}^{T+\Delta T/2} w(t-T) dt =: \bar{w}\Delta T \quad (2.10)$$

## 2.2 Details of specific windows

We will consider different window functions defined on the interval

$$-\frac{1}{2} \leq \frac{t-T}{\Delta T} \leq \frac{1}{2}. \quad (2.11)$$

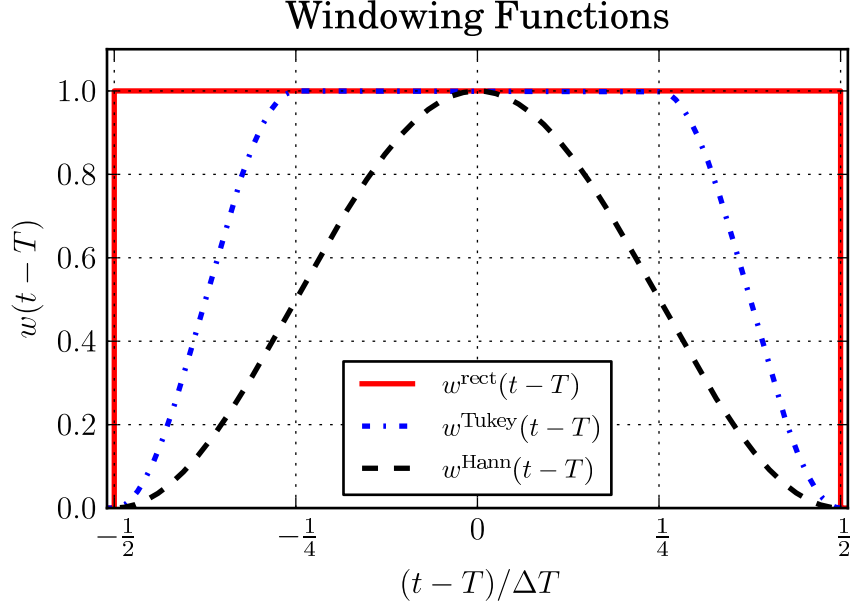
The “unwindowed” case can also be thought of as applying a rectangular window,  $w(t-T) = 1$  on that interval. A Hann window is defined as

$$w^{\text{Hann}}(\xi \Delta T) = \frac{1}{2} (1 + \cos 2\pi \xi) \quad -\frac{1}{2} \leq \xi \leq \frac{1}{2}. \quad (2.12)$$

The default form of the Tukey window looks like two halves of a Hann window with a flat top inserted in between:

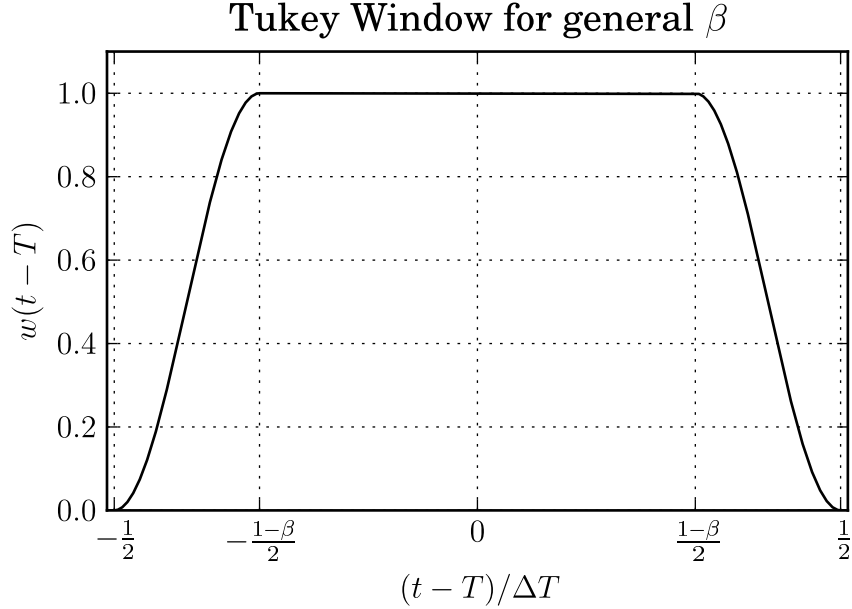
$$w^{\text{Tukey}}(\xi \Delta T) = \begin{cases} \frac{1}{2} (1 - \cos 4\pi \xi) & -\frac{1}{2} \leq \xi \leq -\frac{1}{4} \\ 1 & -\frac{1}{4} \leq \xi \leq \frac{1}{4} \\ \frac{1}{2} (1 - \cos 4\pi \xi) & \frac{1}{4} \leq \xi \leq \frac{1}{2} \end{cases}. \quad (2.13)$$

These three windows are illustrated here:



They are all special cases of the general Tukey window with a parameter  $\beta$  which specifies how much of the window is non-constant:

$$w_{\beta}^{\text{Tukey}}(\xi\Delta T) = \begin{cases} \frac{1}{2} \left( 1 - \cos \frac{\pi}{\beta} (2\xi + 1) \right) & -\frac{1}{2} \leq \xi \leq -\left(\frac{1-\beta}{2}\right) \\ 1 & -\left(\frac{1-\beta}{2}\right) \leq \xi \leq \left(\frac{1-\beta}{2}\right) \\ \frac{1}{2} \left( 1 - \cos \frac{\pi}{\beta} (2\xi - 1) \right) & \left(\frac{1-\beta}{2}\right) \leq \xi \leq \frac{1}{2} \end{cases} \quad (2.14)$$



The Hann window corresponds to  $\beta = 1$ , the rectangular window is  $\beta = 0$ , and the default Tukey window case is  $\beta = 1/2$ . (In this document, when we write Tukey without specifying the  $\beta$  value,  $\beta = 1/2$  is to be understood.)

For each of the windows we can calculate (2.9), which can also be written

$$\delta_{\Delta T}^w(\kappa \delta f) = \Delta T \int_{-1/2}^{1/2} w(\xi \Delta T) e^{-i2\pi\kappa\xi} d\xi \quad (2.15)$$

From the general form (2.14), we can work out

$$\begin{aligned} \frac{\delta_{\Delta T}^w(\kappa \delta f)}{\Delta T} &= \frac{1}{2} \text{sinc } \kappa + \frac{1}{2}(1 - \beta) \text{sinc}(\kappa[1 - \beta]) \\ &\quad + \frac{\beta}{4} \sin \left( \pi \kappa \left[ 1 - \frac{\beta}{2} \right] \right) \left[ \text{sinc} \left( \frac{1 - \beta\kappa}{2} \right) - \text{sinc} \left( \frac{1 + \beta\kappa}{2} \right) \right] \end{aligned} \quad (2.16)$$

where

$$\text{sinc } \alpha = \frac{\sin \pi \alpha}{\pi \alpha} \quad (2.17)$$

is the normalized sinc function. However, it's easier to write (and easier to calculate, in fact) the  $\delta_{\Delta T}^w()$  functions for the three specific windows separately. For the rectangular window ( $\beta = 0$ ), we have

$$\frac{\delta_{\Delta T}(\kappa \Delta T)}{\Delta T} = \text{sinc } \kappa ; \quad (2.18)$$

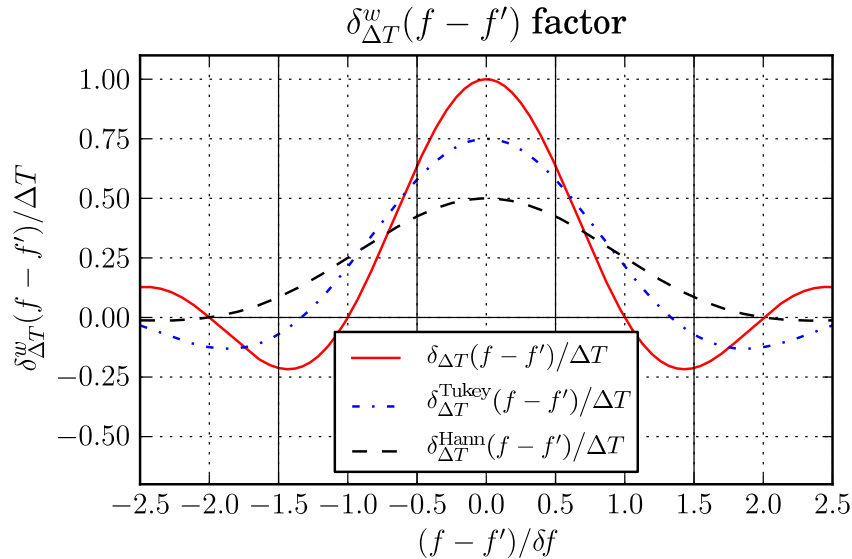
for the Hann window ( $\beta = 1$ ), we have

$$\frac{\delta_{\Delta T}^{\text{Hann}}(\kappa \delta f)}{\Delta T} = \frac{1}{2} \text{sinc } \kappa + \frac{1}{4} \text{sinc}(1 - \kappa) + \frac{1}{4} \text{sinc}(1 + \kappa) ; \quad (2.19)$$

and for the default Tukey window ( $\beta = 1/2$ ), we have

$$\begin{aligned} \frac{\delta_{\Delta T}^{\text{Tukey}}(\kappa \delta f)}{\Delta T} &= \frac{1}{2} \text{sinc } \kappa - \frac{1}{4} \text{sinc}(2 + \kappa) - \frac{1}{4} \text{sinc}(2 - \kappa) \\ &\quad + \frac{1}{4} \text{sinc } \frac{\kappa}{2} + \frac{1}{8} \text{sinc} \left( 1 + \frac{\kappa}{2} \right) + \frac{1}{8} \text{sinc} \left( 1 - \frac{\kappa}{2} \right) \end{aligned} \quad (2.20)$$

We plot these three  $\delta_{\Delta T}^w(f - f')$  functions:



The solid vertical lines, where  $f - f'$  are half-integer multiples of  $\delta f$ , are relevant to the frequency bins of the SFTs. The typical argument of  $\delta_{\Delta T}^w()$  is  $f_k - f_I$ , and for any SFT  $I$  with a signal frequency  $f_I$ , there is some  $k$  value for which  $(f_k - f_I)/\delta f$  is between  $-1/2$  and  $1/2$ . We call that  $k$  value

$$\tilde{k}_I := \left\lfloor \frac{f_I}{\delta f} \right\rfloor = \lfloor f_I \Delta T \rfloor \quad (2.21)$$

and note that whatever the value of

$$\tilde{\kappa}_I = \frac{f_{\tilde{k}_I} - f_I}{\delta f} = \tilde{k}_I - f_I \Delta T, \quad (2.22)$$

each possible value of  $(f_k - f_I)/\delta f = k - f_I \Delta T$  will be  $\tilde{\kappa}_I$  plus some integer.

## 2.3 Signal cross-correlation

Now we consider what happens if we cross-correlate the signal in bin  $k_I$  from SFT  $I$  with bin  $k_J$  from SFT  $J$ . Using (2.8) we find<sup>2</sup>

$$\tilde{h}_{Ik_I}^{w*} \tilde{h}_{Jk_J}^w = h_0^2 \mathcal{G}_{IJ}(-1)^{k_I - k_J} \delta_{\Delta T}^w(f_{k_I} - f_I) \delta_{\Delta T}^w(f_{k_J} - f_J) \quad (2.23)$$

where

$$\mathcal{G}_{IJ} = \frac{1}{4} e^{-i\Delta\Phi_{IJ}} [F_+^I F_+^J \mathcal{A}_+^2 + F_-^I F_-^J \mathcal{A}_-^2 - i(F_+^I F_-^J - F_-^I F_+^J) \mathcal{A}_+ \mathcal{A}_-] \quad (2.24)$$

and

$$\Delta\Phi_{IJ} = \Phi_I - \Phi_J. \quad (2.25)$$

Note that  $\mathcal{G}_{IJ}$  makes no reference to the windowing of the data or to the choice of bins. The “naïve” treatment used in [1, 2] notes that  $\delta_{\Delta T}(0) = \Delta T$  and therefore replaces each of the finite-time delta functions with the SFT length  $\Delta T$ , but for a careful treatment, we must write

$$\frac{\tilde{h}_{Ik_I}^{w*} \tilde{h}_{Jk_J}^w}{(\Delta T)^2} = h_0^2 \mathcal{G}_{Ik_I Jk_J}^w = h_0^2 \mathcal{G}_{IJ}(-1)^{k_I - k_J} \frac{\delta_{\Delta T}^w(f_{k_I} - f_I)}{\Delta T} \frac{\delta_{\Delta T}^w(f_{k_J} - f_J)}{\Delta T} \quad (2.26)$$

or, specialized to rectangular windows,

$$\begin{aligned} \frac{\tilde{h}_{Ik_I}^{w*} \tilde{h}_{Jk_J}^w}{(\Delta T)^2} &= h_0^2 \mathcal{G}_{Ik_I Jk_J}^w = h_0^2 \mathcal{G}_{IJ}(-1)^{k_I - k_J} \frac{\delta_{\Delta T}(f_{k_I} - f_I)}{\Delta T} \frac{\delta_{\Delta T}(f_{k_J} - f_J)}{\Delta T} \\ &= h_0^2 \mathcal{G}_{IJ}(-1)^{k_I - k_J} \text{sinc}([f_{k_I} - f_I]\Delta T) \text{sinc}([f_{k_J} - f_J]\Delta T) \end{aligned} \quad (2.27)$$

If we confine attention to the “best bin” of each SFT, closest to the signal frequency, defined in (2.21), we have

$$\frac{\tilde{h}_{Ik_I}^{w*} \tilde{h}_{Jk_J}^w}{(\Delta T)^2} = h_0^2 \mathcal{G}_{Ik_I Jk_J}^w = h_0^2 \tilde{\mathcal{G}}_{IJ}^w = h_0^2 \mathcal{G}_{IJ}(-1)^{\tilde{k}_I - \tilde{k}_J} \frac{\delta_{\Delta T}^w(f_{\tilde{k}_I} - f_I)}{\Delta T} \frac{\delta_{\Delta T}^w(f_{\tilde{k}_J} - f_J)}{\Delta T} \quad (2.28)$$

---

<sup>2</sup>Compare eq (3.9) of [1].

or, specialized to rectangular windows,

$$\begin{aligned} \frac{\tilde{h}_{I\tilde{k}_I}^* \tilde{h}_{J\tilde{k}_J}}{(\Delta T)^2} &= h_0^2 \mathcal{G}_{I\tilde{k}_I J\tilde{k}_J} = h_0^2 \tilde{\mathcal{G}}_{IJ} = h_0^2 \mathcal{G}_{IJ} (-1)^{\tilde{k}_I - \tilde{k}_J} \frac{\delta_{\Delta T}(f_{\tilde{k}_I} - f_I)}{\Delta T} \frac{\delta_{\Delta T}(f_{\tilde{k}_J} - f_J)}{\Delta T} \\ &= h_0^2 \mathcal{G}_{IJ} (-1)^{\tilde{k}_I - \tilde{k}_J} \text{sinc}([f_{\tilde{k}_I} - f_I]\Delta T) \text{sinc}([f_{\tilde{k}_J} - f_J]\Delta T) \end{aligned} \quad (2.29)$$

If we use the definition (2.22) of  $\tilde{\kappa}_I$  (which ensures  $-\frac{1}{2} \leq \tilde{\kappa}_I \leq \frac{1}{2}$ ) to write

$$(f_k - f_I)\Delta T = k - \tilde{k}_I + \tilde{\kappa}_I, \quad (2.30)$$

we can write the general expected cross-correlation as

$$\mathcal{G}_{Ik_I Jk_J}^w = \mathcal{G}_{IJ} (-1)^{k_I - k_J} \frac{\delta_{\Delta T}^w([k_I - \tilde{k}_I + \tilde{\kappa}_I]\Delta T)}{\Delta T} \frac{\delta_{\Delta T}^w([k_J - \tilde{k}_J + \tilde{\kappa}_J]\Delta T)}{\Delta T} \quad (2.31)$$

which specializes for rectangular windows to

$$\mathcal{G}_{Ik_I Jk_J} = \mathcal{G}_{IJ} (-1)^{k_I - k_J} \text{sinc}(k_I - \tilde{k}_I + \tilde{\kappa}_I) \text{sinc}(k_J - \tilde{k}_J + \tilde{\kappa}_J) \quad (2.32)$$

and the “best bin” expected cross-correlation as

$$\tilde{\mathcal{G}}_{IJ}^w = \mathcal{G}_{I\tilde{k}_I J\tilde{k}_J}^w = \mathcal{G}_{IJ} (-1)^{\tilde{k}_I - \tilde{k}_J} \frac{\delta_{\Delta T}^w(\tilde{\kappa}_I \Delta T)}{\Delta T} \frac{\delta_{\Delta T}^w(\tilde{\kappa}_J \Delta T)}{\Delta T} \quad (2.33)$$

which specializes for rectangular windows to

$$\tilde{\mathcal{G}}_{IJ} = \mathcal{G}_{I\tilde{k}_I J\tilde{k}_J} = \mathcal{G}_{IJ} (-1)^{\tilde{k}_I - \tilde{k}_J} \text{sinc}(\tilde{\kappa}_I) \text{sinc}(\tilde{\kappa}_J). \quad (2.34)$$

## 2.4 Statistics of cross-correlation

Let the data

$$x_I(t) = h_I(t) + n_I(t) \quad (2.35)$$

in SFT  $I$  consist of the signal  $h_I(t)$  plus random instrumental noise  $n_I(t)$  with one-sided power spectral density  $S_I(|f|)$  so that

$$E[n_I(t)] = 0 \quad (2.36)$$

and

$$E[n_I(t)n_J(t')] = \delta_{IJ} \int_{-\infty}^{\infty} \frac{S_I(|f|)}{2} e^{-i2\pi f(t-t')} df. \quad (2.37)$$

If we write the noise contribution to the SFT labelled by  $I$  as

$$\tilde{n}_{Ik}^w = \sum_{j=0}^{N-1} w_j n_{Ij} e^{-i2\pi jk/N} \delta t \approx \int_{T-\Delta T/2}^{T+\Delta T/2} w(t-T) n_I(t) e^{-i2\pi(t-[T-\Delta T/2])f_k} dt \quad (2.38)$$

then (2.36) implies  $E[\tilde{n}_{Ik}^w] = 0$  and we can define a cross-correlation statistic

$$\mathcal{Y}_{Ik_I Jk_J}^w = \frac{\tilde{x}_{Ik_I}^{w*} \tilde{x}_{Jk_J}^w}{(\Delta T)^2} \quad E[\mathcal{Y}_{\alpha\mu}^w] = h_0^2 \mathcal{G}_{\alpha\mu}^w, \quad (2.39)$$



where the index  $\mu$  refers to the pair of frequency bins chosen from the SFT pair  $\alpha$ . Specialized to rectangular windows, we write

$$\mathcal{Y}_{I k_I J k_J} = \frac{\tilde{x}_{I k_I}^* \tilde{x}_{J k_J}}{(\Delta T)^2} ; \quad E[\mathcal{Y}_{\alpha\mu}] = h_0^2 \mathcal{G}_{\alpha\mu} . \quad (2.40)$$

If we take the “best bin” from each SFT, we have

$$\tilde{\mathcal{Y}}_{IJ}^w = \mathcal{Y}_{I \tilde{k}_I J \tilde{k}_J}^w = \frac{\tilde{x}_{I \tilde{k}_I}^{w*} \tilde{x}_{J \tilde{k}_J}^w}{(\Delta T)^2} ; \quad E[\tilde{\mathcal{Y}}_\alpha^w] = h_0^2 \tilde{\mathcal{G}}_\alpha^w , \quad (2.41)$$

or, specialized to rectangular windows,

$$\tilde{\mathcal{Y}}_{IJ} = \mathcal{Y}_{I \tilde{k}_I J \tilde{k}_J} = \frac{\tilde{x}_{I \tilde{k}_I}^* \tilde{x}_{J \tilde{k}_J}}{(\Delta T)^2} ; \quad E[\tilde{\mathcal{Y}}_\alpha] = h_0^2 \tilde{\mathcal{G}}_\alpha . \quad (2.42)$$

In the low-signal limit  $h_0 \ll S_I(f_{\tilde{k}_I})\Delta T$ , the variances (and potentially covariances) will be determined by the statistics of the noise. We can use (2.37) to show

$$\begin{aligned} E[\tilde{n}_{I k}^{w*} \tilde{n}_{J k'}^w] &= \delta_{IJ} (-1)^{k-k'} \int_{-\infty}^{\infty} \frac{S_I(|f|)}{2} \delta_{\Delta T}^{w*}(f_k - f) \delta_{\Delta T}^w(f_{k'} - f) df \\ &\approx \delta_{IJ} (-1)^{k-k'} \frac{S_I(f_I)}{2} \int_{-\infty}^{\infty} \delta_{\Delta T}^{w*}(f_k - f) \delta_{\Delta T}^w(f_{k'} - f) df \end{aligned} \quad (2.43)$$

Using (2.9) we can show

$$\begin{aligned} \int_{-\infty}^{\infty} \delta_{\Delta T}^{w*}(f_k - f) \delta_{\Delta T}^w(f_{k'} - f) df &= \int_{T-\Delta T/2}^{T+\Delta T/2} e^{i2\pi(f_k - f_{k'})(t-T)} [w(t-T)]^2 dt \\ &= \Delta T \int_{-1/2}^{1/2} e^{i2\pi\xi(k-k')} [w(\xi\Delta T)]^2 d\xi \end{aligned} \quad (2.44)$$

In particular, for the “diagonal” term  $k = k'$ , this is

$$\int_{-\infty}^{\infty} |\delta_{\Delta T}^w(f_k - f)|^2 df = \int_{T-\Delta T/2}^{T+\Delta T/2} [w(t-T)]^2 dt = \Delta T \overline{w^2} , \quad (2.45)$$

so that

$$E[\tilde{n}_{I \tilde{k}_I}^{w*} \tilde{n}_{J \tilde{k}_J}^w] \approx \delta_{IJ} \frac{S_I(f_I)}{2} \Delta T \overline{w^2} \quad (2.46)$$

For the special case of rectangular windows, the diagonal term is the only one there is:

$$\int_{-\infty}^{\infty} \delta_{\Delta T}^*(f_k - f) \delta_{\Delta T}(f_{k'} - f) df = \Delta T \int_{-1/2}^{1/2} e^{i2\pi\xi(k-k')} d\xi = \Delta T \text{sinc}(k - k') = \Delta T \delta_{kk'} , \quad (2.47)$$

so that

$$E[\tilde{n}_{I k}^* \tilde{n}_{J k'}] \approx \delta_{IJ} \delta_{kk'} \frac{S_I(f_I)}{2} \Delta T \quad (2.48)$$

In general, though,

$$E [\tilde{n}_{Ik}^{w*} \tilde{n}_{Jk'}^w] \approx \delta_{IJ} \frac{S_I(f_I)}{2} \Delta T (-1)^{k-k'} \int_{-1/2}^{1/2} e^{i2\pi\xi(k-k')} [w(\xi\Delta T)]^2 d\xi =: \delta_{IJ} \frac{S_I(f_I)}{2} \Delta T \gamma_{kk'}^w \quad (2.49)$$

Using (2.46), we can show that, in the low-signal limit,

$$\text{Cov}(\tilde{\mathcal{Y}}_\alpha^w, \tilde{\mathcal{Y}}_\beta^w) = \delta_{\alpha\beta} \text{Var} \tilde{\mathcal{Y}}_\alpha^w \quad (2.50)$$

where the variance is

$$\text{Var} \tilde{\mathcal{Y}}_{IJ}^w \approx \frac{E [\tilde{n}_{Ik_I}^{w*} \tilde{n}_{Ik_I}^w]}{(\Delta T)^2} \frac{E [\tilde{n}_{Jk_J}^{w*} \tilde{n}_{Jk_J}^w]}{(\Delta T)^2} = \frac{S_I(f_I) S_J(f_J)}{4} \frac{(\overline{w^2})^2}{(\Delta T)^2} =: \sigma_{IJ}^{w^2} \quad (2.51)$$

if we write the rectangular windowed case as

$$\text{Var} \tilde{\mathcal{Y}}_{IJ} \approx \frac{S_I(f_I) S_J(f_J)}{4(\Delta T)^2} =: \sigma_{IJ}^2 \quad (2.52)$$

this means that

$$\text{Cov}(\tilde{\mathcal{Y}}_\alpha^w, \tilde{\mathcal{Y}}_\beta^w) = \delta_{\alpha\beta} \sigma_\alpha^{w^2} = \delta_{\alpha\beta} (\overline{w^2})^2 \sigma_\alpha^2 \quad (2.53)$$

If we now consider the statistic  $\mathcal{Y}_{Ik_I Jk_J}$  constructed from arbitrary bins of rectangular-windowed SFTs, (2.48) shows that different statistics are still uncorrelated, so

$$\text{Cov}(\mathcal{Y}_{\alpha\mu}, \mathcal{Y}_{\beta\nu}) = \delta_{\alpha\beta} \delta_{\mu\nu} \text{Var} \mathcal{Y}_{\alpha\mu} \quad (2.54)$$

with the variance

$$\text{Var} \mathcal{Y}_{Ik_I Jk_J} \approx \frac{E [\tilde{n}_{Ik_I}^{w*} \tilde{n}_{Ik_I}^w]}{(\Delta T)^2} \frac{E [\tilde{n}_{Jk_J}^{w*} \tilde{n}_{Jk_J}^w]}{(\Delta T)^2} = \frac{S_I(f_I) S_J(f_J)}{4(\Delta T)^2} = \sigma_{IJ}^2 \quad (2.55)$$

i.e.,

$$\text{Cov}(\mathcal{Y}_{\alpha\mu}, \mathcal{Y}_{\beta\nu}) = \delta_{\alpha\beta} \delta_{\mu\nu} \sigma_\alpha^2 \quad (2.56)$$

For the fully general statistic  $\mathcal{Y}_{Ik_I Jk_J}^w$ , noise in different bins of the same SFT will be correlated, so

$$\text{Cov}(\mathcal{Y}_{Ik_I Jk_J}^w, \mathcal{Y}_{Ik'_I Jk'_J}^w) \approx E [\tilde{n}_{Ik_I}^w \tilde{n}_{Ik'_I}^{w*}] E [\tilde{n}_{Jk_J}^{w*} \tilde{n}_{Jk'_J}^w] \approx \sigma_{IJ}^2 \gamma_{Ik_I k'_I}^w \gamma_{Jk_J k'_J}^w \quad (2.57)$$

where

$$\gamma_{kk'}^w = (-1)^{k-k'} \int_{-1/2}^{1/2} e^{i2\pi\xi(k-k')} [w(\xi\Delta T)]^2 d\xi \quad (2.58)$$

and, if we write

$$\Gamma_{Ik_I k'_I Jk_J k'_J}^w = \gamma_{Ik_I k'_I}^w \gamma_{Jk_J k'_J}^w \quad (2.59)$$

we can write this compactly as

$$\text{Cov}(\mathcal{Y}_{\alpha\mu}^w, \mathcal{Y}_{\beta\nu}^w) = \delta_{\alpha\beta} \Gamma_{\mu\nu}^w \sigma_\alpha^2 \quad (2.60)$$

## 2.5 Optimal combination

In the case of the best-bin search, where the cross-correlation statistics  $\{\tilde{\mathcal{Y}}_\alpha^w\}$  from the various SFT pairs can be treated as independent random variables with mean and variance

$$E[\tilde{\mathcal{Y}}_\alpha^w] = h_0^2 \tilde{\mathcal{G}}_\alpha^w \quad \text{Var } \tilde{\mathcal{Y}}_\alpha^w = \sigma_\alpha^{w2} \quad (2.61)$$

the optimal real linear combination of those statistics will be

$$\rho = \left( 2 \sum_\beta \frac{|\tilde{\mathcal{G}}_\beta^w|^2}{\sigma_\beta^{w2}} \right)^{-1/2} \sum_\alpha \frac{\tilde{\mathcal{G}}_\alpha^{w*} \mathcal{Y}_\alpha^w + \tilde{\mathcal{G}}_\alpha^w \mathcal{Y}_\alpha^{w*}}{\sigma_\alpha^{w2}} \quad (2.62)$$

which implies that

$$E[\rho] = h_0^2 \left( 2 \sum_\beta \frac{|\tilde{\mathcal{G}}_\beta^w|^2}{\sigma_\beta^{w2}} \right)^{1/2} \quad (2.63a)$$

$$\text{Var } \rho = 1 \quad (2.63b)$$

For a multi-bin rectangular-windowed search, we still have a set of independent cross-correlation statistics  $\{\mathcal{Y}_{\alpha\mu}^w\}$  with mean and variance

$$E[\mathcal{Y}_{\alpha\mu}^w] = h_0^2 \mathcal{G}_{\alpha\mu} \quad \text{Var } \mathcal{Y}_{\alpha\mu}^w = \sigma_\alpha^2 \quad (2.64)$$

so the optimal combination is

$$\rho = \left( 2 \sum_\beta \frac{\sum_\nu |\mathcal{G}_{\beta\nu}|^2}{\sigma_\beta^2} \right)^{-1/2} \sum_\alpha \frac{\sum_\mu (\mathcal{G}_{\alpha\mu}^* \mathcal{Y}_{\alpha\mu}^w + \mathcal{G}_{\alpha\mu} \mathcal{Y}_{\alpha\mu}^{w*})}{\sigma_\alpha^2} \quad (2.65)$$

which implies that

$$E[\rho] = h_0^2 \left( 2 \sum_\beta \frac{\sum_\nu |\mathcal{G}_{\beta\nu}|^2}{\sigma_\beta^2} \right)^{1/2} \quad (2.66a)$$

$$\text{Var } \rho = 1 \quad (2.66b)$$

Finally, if we wish to combine cross-correlation statistics using multiple bins from windowed SFTs, we have to deal with the fact that the statistics involving different pairs of bins from the same pair of SFTs will be correlated:

$$E[\mathcal{Y}_{\alpha\mu}^w] = h_0^2 \mathcal{G}_{\alpha\mu}^w \quad \text{Cov}(\mathcal{Y}_{\alpha\mu}^w, \mathcal{Y}_{\beta\nu}^w) = \delta_{\alpha\beta} \Gamma_{\mu\nu}^w \sigma_\alpha^2 \quad (2.67)$$

This means that, in order to produce the optimal combination

$$\rho = \left( 2 \sum_\beta \frac{\sum_{\lambda\sigma} (\Gamma_w^{-1})_{\lambda\sigma} \mathcal{G}_{\beta\lambda}^{w*} \mathcal{G}_{\beta\sigma}^w}{\sigma_\beta^2} \right)^{-1/2} \sum_\alpha \frac{\sum_\mu \sum_\nu (\Gamma_w^{-1})_{\mu\nu} (\mathcal{G}_{\alpha\mu}^{w*} \mathcal{Y}_{\alpha\nu}^w + \mathcal{G}_{\alpha\mu}^w \mathcal{Y}_{\alpha\nu}^{w*})}{\sigma_\alpha^2} \quad (2.68)$$

we need the inverse matrix  $\{(\Gamma_w^{-1})_{\mu\nu}\}$  which comes from inverting the matrix  $\{\gamma_{kk'}^w\}$  defined in (2.58):

$$(\Gamma_w^{-1})_{k_I k_J k'_I k'_J} = (\gamma_w^{-1})_{k_I k'_I} (\gamma_w^{-1})_{k_J k'_J} . \quad (2.69)$$

This then produces a statistic with the following mean and variance:

$$E[\rho] = h_0^2 \left( 2 \sum_{\beta} \frac{\sum_{\lambda\sigma} (\Gamma_w^{-1})_{\lambda\sigma} \mathcal{G}_{\beta\lambda}^{w*} \mathcal{G}_{\beta\sigma}^w}{\sigma_{\beta}^2} \right)^{1/2} \quad (2.70a)$$

$$\text{Var } \rho = 1 \quad (2.70b)$$

### 3 Sensitivity estimates for different windowing options

#### 3.1 Naïve sensitivity

The sensitivity estimates in [1] and [2] are based on the assumption that

$$E[\rho] = h_0^2 \left( 2 \sum_{\alpha} \frac{|\mathcal{G}_{\alpha}|^2}{\sigma_{\alpha}^2} \right)^{1/2} \quad (3.1)$$

which ignores the factors arising from windowing and leakage. This “naïve” formula results in an overestimate of the expected signal-to-noise of the search.

#### 3.2 Best-bin sensitivities

We calculate the expectation value of  $\rho$  by taking the contributions from only the “best” bins (2.21) and using (2.28)

$$\tilde{\mathcal{G}}_{IJ}^w = \mathcal{G}_{IJ} (-1)^k \frac{\delta_{\Delta T}^{w*}(f_{\tilde{k}_I} - f_I)}{\Delta T} \frac{\delta_{\Delta T}^w(f_{\tilde{k}_J} - f_J)}{\Delta T} . \quad (3.2)$$

and, from (2.51),

$$\sigma_{IJ}^{w^2} = \frac{S_I(f_{\tilde{k}_I}) S_J(f_{\tilde{k}_J}) (\overline{w^2})^2}{4 (\Delta T)^2} = \sigma_{IJ}^2 (\overline{w^2})^2 \quad (3.3)$$

So

$$E[\rho] = h_0^2 \left( 2 \sum_{IJ} \frac{|\tilde{\mathcal{G}}_{IJ}^w|^2}{\sigma_{IJ}^{w^2}} \right)^{1/2} = h_0^2 \left( 2 \sum_{IJ} \frac{|\mathcal{G}_{IJ}|^2}{\sigma_{IJ}^2} \frac{1}{(\overline{w^2})^2} \left| \frac{\delta_{\Delta T}^w(f_{\tilde{k}_I} - f_I)}{\Delta T} \right|^2 \left| \frac{\delta_{\Delta T}^w(f_{\tilde{k}_J} - f_J)}{\Delta T} \right|^2 \right)^{1/2} \quad (3.4)$$

##### 3.2.1 Upper bound

For a symmetric, monotonic, non-negative window

$$\delta_{\Delta T}^w(f_{\tilde{k}_I} - f_I) \leq \delta_{\Delta T}^w(0) = \Delta T \overline{w} , \quad (3.5)$$

we have the limit

$$E[\rho] \leq \frac{(\bar{w})^2}{(w^2)} h_0^2 \left( 2 \sum_{IJ} \frac{|\mathcal{G}_{IJ}|^2}{\sigma_{IJ}^2} \right)^{1/2} \quad (3.6)$$

For the rectangular window, this prefactor of  $\frac{(\bar{w})^2}{(w^2)}$  is 1, For Hann window it is

$$\frac{(1/2)^2}{3/8} = \frac{2}{3} = \sqrt{\frac{4}{9}} \quad (3.7)$$

while for Tukey, it is

$$\frac{(3/4)^2}{11/16} = \frac{9}{11} = \sqrt{\frac{81}{121}} \quad (3.8)$$

For a general Tukey window with arbitrary  $\beta$ , it is

$$\frac{(1 - \beta/2)^2}{1 - 5\beta/8} = \frac{8 - 8\beta + 2\beta^2}{8 - 5\beta} \quad (3.9)$$

Hence for rectangular windows the upper limit of the expectation value of  $\rho$  is same as that of the naïve sensitivity, whereas for Hann it is 2/3 and 9/11 times that of the naïve sensitivity respectively.

### 3.2.2 Averaged values

Assuming that the sum over pairs evenly samples the possible values of  $\kappa = (f_{\bar{k}_I} - f_I)\Delta T$  and  $\kappa' = (f_{\bar{k}_J} - f_J)\Delta T$  we expect the actual reduction due to using the best bin from windowed data will be

$$\begin{aligned} E[\rho] &\approx h_0^2 \left( \frac{1}{(w^2)^2} \left\langle \left| \frac{\delta_{\Delta T}^w(\kappa \delta f)}{\Delta T} \right|^2 \right\rangle_{\kappa} \left\langle \left| \frac{\delta_{\Delta T}^w(\kappa' \delta f)}{\Delta T} \right|^2 \right\rangle_{\kappa'} 2 \sum_{IJ} \frac{|\mathcal{G}_{IJ}|^2}{\sigma_{IJ}^2} \right)^{1/2} \\ &= h_0^2 \frac{1}{(w^2)} \left\langle \left| \frac{\delta_{\Delta T}^w(\kappa \delta f)}{\Delta T} \right|^2 \right\rangle_{\kappa} \left( 2 \sum_{IJ} \frac{|\mathcal{G}_{IJ}|^2}{\sigma_{IJ}^2} \right)^{1/2} \end{aligned} \quad (3.10)$$

For each of the windows, we compare the estimate of

$$E[\rho] \approx h_0^2 \frac{1}{(w^2)} \left\langle \left| \frac{\delta_{\Delta T}^w(\kappa \delta f)}{\Delta T} \right|^2 \right\rangle_{\kappa} \left( 2 \sum_{IJ} \frac{|\mathcal{G}_{IJ}|^2}{\sigma_{IJ}^2} \right)^{1/2} \quad (3.11)$$

to the upper limit

$$E[\rho]_{\max} = \frac{(\bar{w})^2}{(w^2)} h_0^2 \left( 2 \sum_{IJ} \frac{|\mathcal{G}_{IJ}|^2}{\sigma_{IJ}^2} \right)^{1/2} \quad (3.12)$$

and the “naïve” expression

$$E[\rho]_{\text{naïve}} = h_0^2 \left( 2 \sum_{IJ} \frac{|\mathcal{G}_{IJ}|^2}{\sigma_{IJ}^2} \right)^{1/2} \quad (3.13)$$

Window	rect	Tukey	Hann
$E[\rho]_{\max} / E[\rho]_{\text{naïve}}$	1.000	0.818	0.667
$E[\rho] / E[\rho]_{\text{naïve}}$	0.774	0.699	0.601
$E[\rho] / E[\rho]_{\max}$	0.774	0.854	0.901

We see that while rectangular windows suffer greater leakage and fractional reduction of SNR relative to their upper bound, the fact that upper bound is higher means that they still give the best single-bin sensitivity.

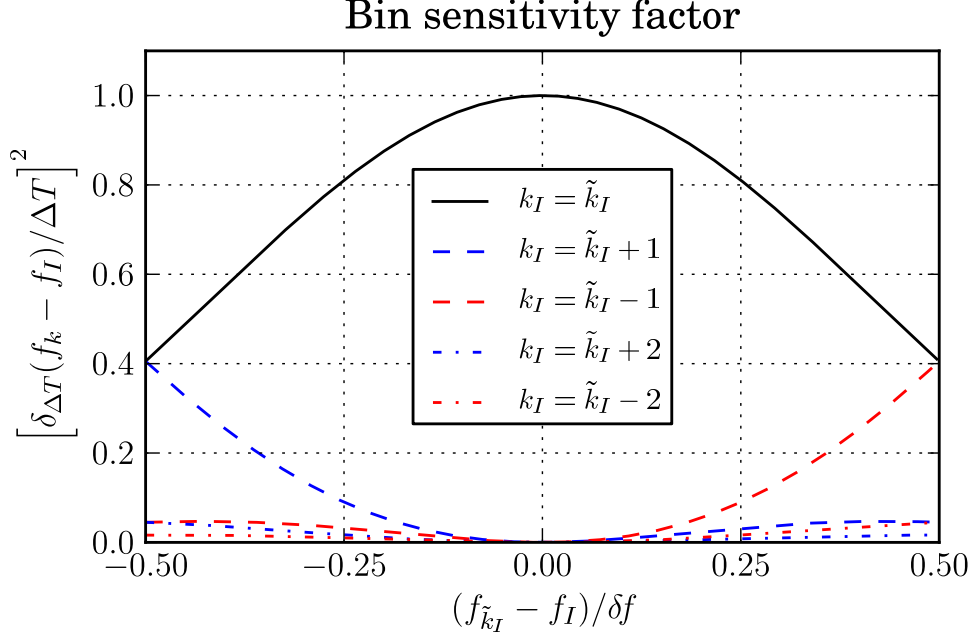
### 3.3 Multiple-bin sensitivities

We saw in section 2.5 that the contributions from multiple bins could be combined into a single detection statistic.

We limit attention to the case of rectangular windows, where the contributions from multiple bins can simple be combined to get

$$\begin{aligned}
E[\rho] &= h_0^2 \left( 2 \sum_{IJ} \sum_{k_I \in \mathcal{K}_I} \sum_{k_J \in \mathcal{K}_J} \frac{|\tilde{\mathcal{G}}_{Ik_I Jk_J}|^2}{\sigma_{IJ}^2} \right)^{1/2} \\
&= h_0^2 \left( 2 \sum_{IJ} \frac{|\mathcal{G}_{IJ}|^2}{\sigma_{IJ}^2} \sum_{k_I \in \mathcal{K}_I} \left[ \frac{\delta_{\Delta T}(f_{k_I} - f_I)}{\Delta T} \right]^2 \sum_{k_J \in \mathcal{K}_J} \left[ \frac{\delta_{\Delta T}(f_{k_J} - f_J)}{\Delta T} \right]^2 \right)^{1/2} \\
&= h_0^2 \left( 2 \sum_{IJ} \frac{|\mathcal{G}_{IJ}|^2}{\sigma_{IJ}^2} \sum_{k_I \in \mathcal{K}_I} \text{sinc}^2([f_{k_I} - f_I]\Delta T) \sum_{k_J \in \mathcal{K}_J} \text{sinc}^2([f_{k_J} - f_J]\Delta T) \right)^{1/2}
\end{aligned} \tag{3.14}$$

For a particular pair of SFTs, the factors  $\sum_{k_I \in \mathcal{K}_I} \text{sinc}^2([f_{k_I} - f_I]\Delta T)$  and  $\sum_{k_J \in \mathcal{K}_J} \text{sinc}^2([f_{k_J} - f_J]\Delta T)$  will depend on how close the Doppler shifted frequencies  $f_I$  and  $f_J$  are to the “best bin” frequencies  $f_{\tilde{k}_I}$  and  $f_{\tilde{k}_J}$ . The contributions from the most sensitive few bins look like this:



Note that no matter the value of  $(f_{\tilde{k}_J} - f_J)\Delta T$ ,

$$\sum_{k_I \in \mathcal{K}_I} \text{sinc}^2([f_{k_I} - f_I]\Delta T) = \sum_{k_I \in \mathcal{K}_I} \text{sinc}^2([f_{\tilde{k}_I} - f_I]\Delta T + [k_I - \tilde{k}_I]) \leq 1, \quad (3.15)$$

because of the identity<sup>3</sup>  $\sum_{s=-\infty}^{\infty} \text{sinc}^2(\kappa + s) = 1$ , valid for any  $\kappa$ . If we assume that, over the course of an observation,  $(f_{\tilde{k}_I} - f_I)\Delta T$  and  $(f_{\tilde{k}_J} - f_J)\Delta T$  evenly sample the range of possible values from  $-\frac{1}{2}$  to  $\frac{1}{2}$ , in a way that's uncorrelated with the value of  $\mathcal{G}_{IJ}$ , we can approximate

$$\begin{aligned} E[\rho] &= h_0^2 \left( 2 \sum_{IJ} \frac{|\mathcal{G}_{IJ}|^2}{\sigma_{IJ}^2} \sum_{k_I \in \mathcal{K}_I} \text{sinc}^2([f_{k_I} - f_I]\Delta T) \sum_{k_J \in \mathcal{K}_J} \text{sinc}^2([f_{k_J} - f_J]\Delta T) \right)^{1/2} \\ &\approx h_0^2 \left( 2 \sum_{IJ} \frac{|\mathcal{G}_{IJ}|^2}{\sigma_{IJ}^2} \left\langle \sum_s \text{sinc}^2(\kappa + s) \right\rangle_{\kappa} \left\langle \sum_{s'} \text{sinc}^2(\kappa' + s') \right\rangle_{\kappa'} \right)^{1/2} \\ &= h_0^2 \left( 2 \sum_{\alpha} \frac{|\mathcal{G}_{\alpha}|^2}{\sigma_{\alpha}^2} \right)^{1/2} \sum_s \langle \text{sinc}^2(\kappa + s) \rangle_{\kappa} \end{aligned} \quad (3.16)$$

where  $\sum_s$  indicates a sum over the possible integer bin offsets and  $\langle \cdot \rangle_{\kappa}$  indicates an average over the possible offsets within the bin. Specifically, if we take the  $m$  bins whose centers are closest to the Doppler-shifted frequencies,

$$\sum_s \langle \text{sinc}^2(\kappa + s) \rangle_{\kappa} = \sum_{s=-\lceil(m-1)/2\rceil}^{\lfloor(m-1)/2\rfloor} 2 \int_0^{1/2} \text{sinc}^2(\kappa + s) d\kappa = 2 \int_0^{m/2} \text{sinc}^2 \kappa d\kappa \quad (3.17)$$

We summarize these estimates here:

<sup>3</sup>This is most easily proved by writing  $\text{sinc}(\kappa + s) = \int_{-1/2}^{1/2} e^{i2\pi(\kappa+s)t} dt$  and using  $\sum_{s=-\infty}^{\infty} e^{i2\pi s(t-t')} = \sum_{s=-\infty}^{\infty} \delta(t - t' + s)$ .

$m$	1	2	3	4	5	6	7	8	9
contribution	0.774	0.129	0.028	0.019	0.009	0.007	0.005	0.004	0.003
cumulative	0.774	0.903	0.931	0.950	0.959	0.966	0.971	0.975	0.977

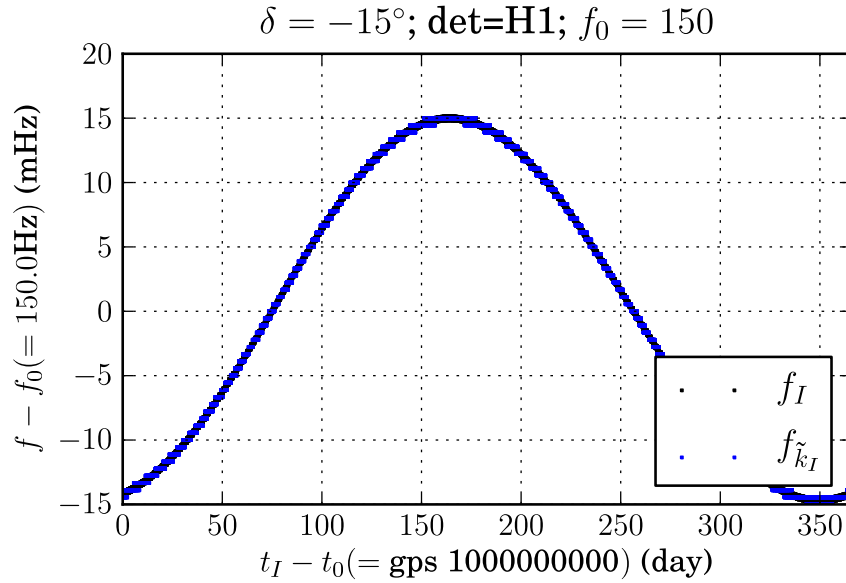
### 3.4 Examples with specific parameter choices

To investigate the effectiveness of the hypothesized average over  $\kappa$ , we examine some specific choices of SFT times. We make the simplifying assumption, introduced in [1], of replacing  $\mathcal{G}_{IJ}$  with its average over  $\cos \iota$  (from  $-1$  to  $1$ ) and  $\psi$  (from  $0$  to  $\pi$ ); under that average,

$$\mathcal{G}_\beta \longrightarrow \mathcal{G}_{IJ}^{\text{ave}} = \frac{1}{10} e^{-i\Delta\Phi_{IJ}} (a^I a^J + b^I b^J) \quad (3.18)$$

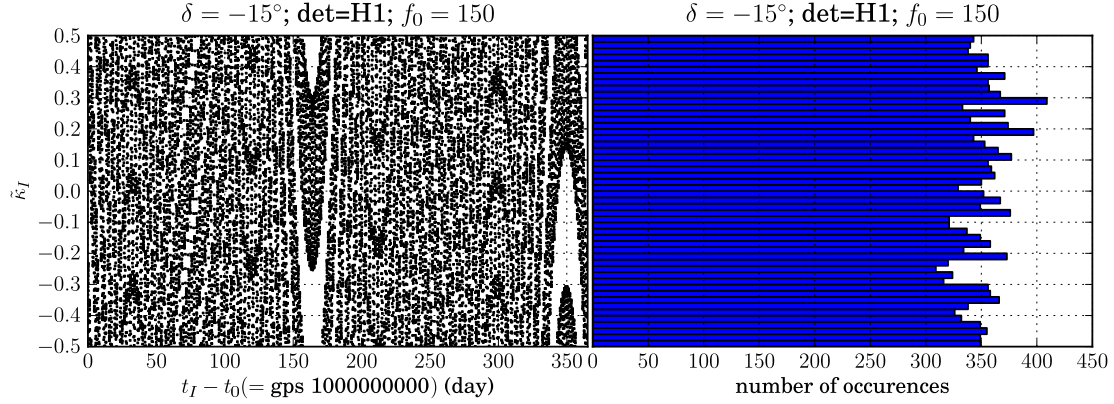
where  $a^I$  and  $b^I$  are the amplitude modulation factors[3] and depend only on the SFT (detector and sidereal time) and sky position.

Here in the section, we check if the values in the 2 tables which we got theoretically using the averaged templates match with simulated data and numerically performing the entire calculation without any averaging assumed. We initially consider a monochromatic source at the sky position of Sco X-1, without any binary Doppler modulation. To get a look at the variation of the received signal frequency due to the daily and annual Doppler shift, consider the case where  $f_0 = 150$  Hz:

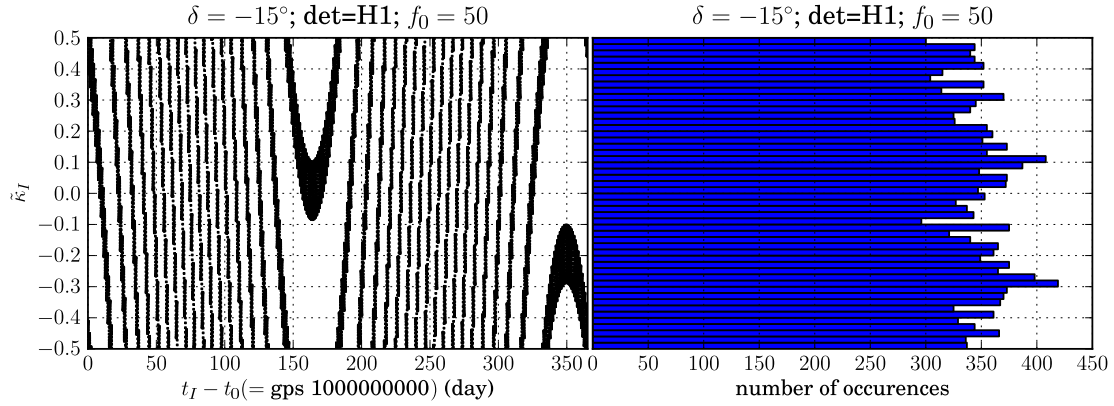


We can look at the scatter and histogram of the  $\tilde{\kappa}_I$  values and see that it is mostly spread out throughout the year:

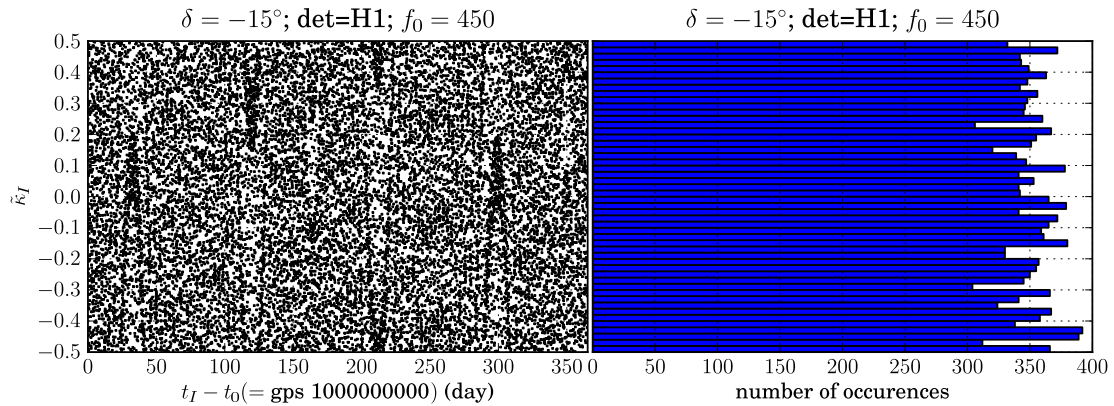




If the signal frequency is  $f_0 = 50$  Hz so that the fractional Doppler shift works out to fewer bins, we see more structure and a less uniform average.



If the signal frequency is  $f_0 = 450$  Hz we see that the structure washes out and the average is rather good:



Now we look at the multiple bin cross correlation sensitivity statistic examples. The default parameters are the following

- A year's worth of data

- Signal frequency  $f_0 = 150$  Hz
- SFT duration is  $\Delta T = 1800$  s
- The maximum allowed offset lag is 3 hours
- The H1 and L1 detectors are involved.

With the default parameters we get the following results (R, T or H refer to rectangular, Tukey and Hann windows respectively, and R1, R2, etc refer to a search which combines the 1, 2, etc best bins from each SFT):

Window	naive	R1	H1	T1	R2	R3
$E[\rho] / E[\rho]_{\text{naive}}$	1.000	0.783	0.602	0.702	0.903	0.931
$E[\rho] / \left( h_0^2 \Delta T / \sqrt{S_I(f_0) S_J(f_0)} \right)$	37.812	29.605	22.745	26.528	34.156	35.210

If we restrict attention to only SFTs from one detector, L1, and keep the remaining parameters the same, we get

Window	naive	R1	H1	T1	R2	R3
$E[\rho] / E[\rho]_{\text{naive}}$	1.000	0.788	0.602	0.703	0.903	0.931
$E[\rho] / \left( h_0^2 \Delta T / \sqrt{S_I(f_0) S_J(f_0)} \right)$	31.005	24.431	18.652	21.784	27.993	28.856

If we use 4 months worth of data from H1 and L1 instead of a year and keep the remaining parameters the same.

Window	naive	R1	H1	T1	R2	R3
$E[\rho] / E[\rho]_{\text{naive}}$	1.000	0.784	0.602	0.702	0.904	0.932
$E[\rho] / \left( h_0^2 \Delta T / \sqrt{S_I(f_0) S_J(f_0)} \right)$	21.662	16.987	13.040	15.214	19.579	20.180

If we change the signal frequency  $f_0$  to 50 Hz instead and use the defaults for the other parameters, we get

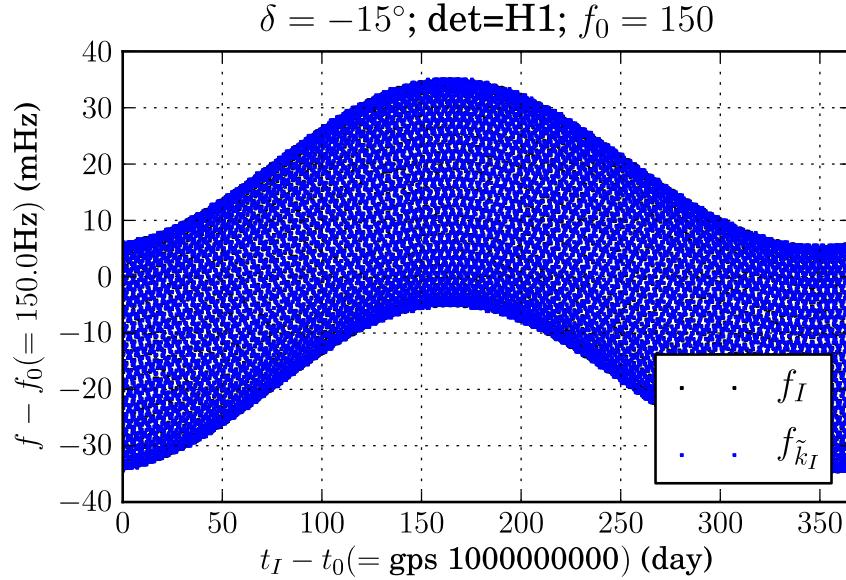
Window	naive	R1	H1	T1	R2	R3
$E[\rho] / E[\rho]_{\text{naive}}$	1.000	0.798	0.605	0.708	0.906	0.933
$E[\rho] / \left( h_0^2 \Delta T / \sqrt{S_I(f_0) S_J(f_0)} \right)$	37.812	30.165	22.860	26.768	34.267	35.289

If the signal frequency  $f_0$  is 450 Hz and the other parameters have their default values, we see

Window	naive	R1	H1	T1	R2	R3
$E[\rho] / E[\rho]_{\text{naive}}$	1.000	0.767	0.600	0.697	0.902	0.931
$E[\rho] / \left( h_0^2 \Delta T / \sqrt{S_I(f_0) S_J(f_0)} \right)$	37.812	29.016	22.700	26.366	34.121	35.201

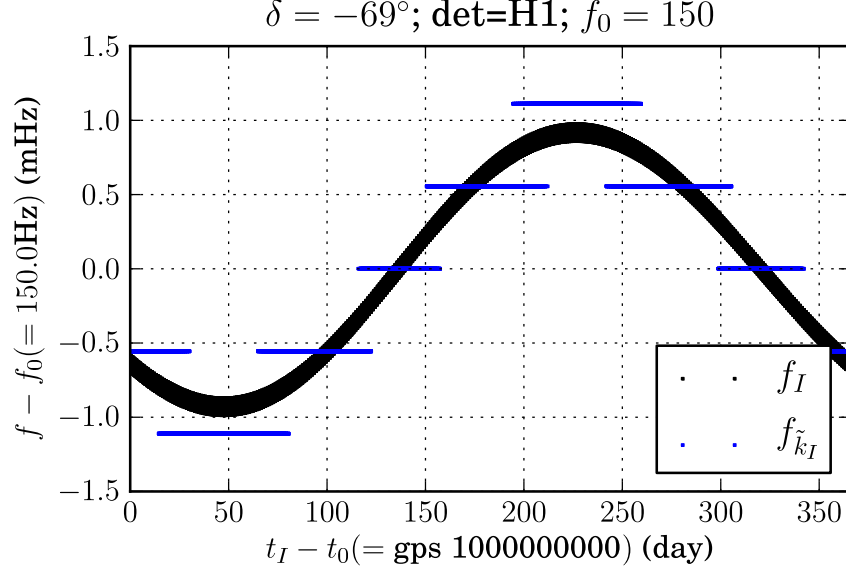
### 3.4.1 Caveats

Our results seem to show that the sensitivity impacts of windowing and leakage are close to the values we approximated by assuming an average over  $\kappa$  values. However, the example of an isolated neutron star at the Sco X-1 location was a bit artificial. For instance, if we include the Doppler modulation to Sco X-1's best-fit binary orbital parameters, we get a rather different looking frequency vs time plot:

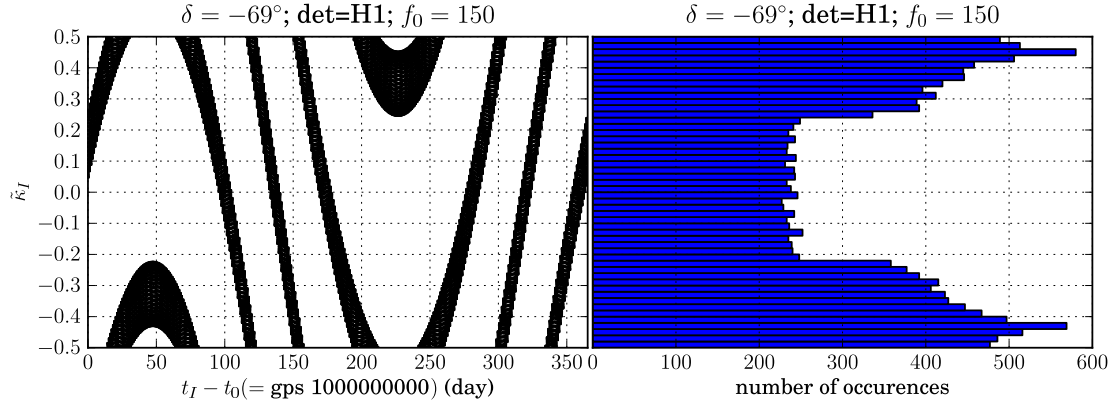


This should average even better over  $\tilde{\kappa}$ , but brings up its own issues. For instance, the assumed choice of 30-minute SFTs will not be enough to track the rapid changes in Doppler-shifted frequencies, so shorter SFTs will be used, and in the process the best-bin frequencies will be spaced further apart.

Finally, the approximate  $\tilde{\kappa}$  averaging is in part a consequence of the sky position of Sco X-1 being close to the ecliptic plane. If we look at a monochromatic source in the sky position of SN1987A, we find a rather different frequency behavior:



with the result that the distribution of  $\tilde{\kappa}$  values is not at all uniform:



We have not yet investigated the consequences of this on the best-bin and multi-bin sensitivity estimates.

## References

- [1] Sanjeev Dhurandhar, Badri Krishnan, Himan Mukhopadhyay, and John T. Whelan. The cross-correlation search for periodic gravitational waves. *Phys. Rev. D*, 77:082001, 2008.
- [2] Christine Chung, Andrew Melatos, Badri Krishnan, and John T. Whelan. Designing a cross-correlation search for continuous-wave gravitational radiation from a neutron star in the supernova remnant SNR 1987A. *Mon. Not. R. Astron. Soc.*, 414:2650–2663, 2011.
- [3] Piotr Jaranowski, Andrzej Krolak, and Bernard F. Schutz. Data analysis of gravitational-wave signals from spinning neutron stars. I: The signal and its detection. *Phys. Rev. D*, 58:063001, 1998.